Low-frequency Accelerometer Based on Molecular Electronic Transducer in Galvanic Cell

by

Zuofeng Zhao

A Dissertation Presented in Partial Fulfillment
of the Requirements for the Degree
Master of Science

Approved November 2015 by the
Graduate Supervisory Committee:

Hongyu Yu, Co-Chair
Junshan Zhang, Co-Chair
Hanqing Jiang

ARIZONA STATE UNIVERSITY

December 2015

ABSTRACT

In this thesis, an approach to develop low-frequency accelerometer based on molecular electronic transducers (MET) in an electrochemical cell is presented. Molecular electronic transducers are a class of inertial sensors which are based on an electrochemical mechanism. Motion sensors based on MET technology consist of an electrochemical cell that can be used to detect the movement of liquid electrolyte between electrodes by converting it to an output current. Seismometers based on MET technology are attractive for planetary applications due to their high sensitivity, low noise, small size and independence on the direction of sensitivity axis. In addition, the fact that MET based sensors have a liquid inertial mass with no moving parts makes them rugged and shock tolerant (basic survivability has been demonstrated to >20 kG).

A Zn-Cu electrochemical cell (Galvanic cell) was applied in the low-frequency accelerometer. Experimental results show that external vibrations (range from 18 to 70 Hz) were successfully detected by this accelerometer as reactions $Zn \rightarrow Zn^{2+} + 2e^{-}$ occurs around the anode and $Cu^{2+} + 2e^{-} \rightarrow Cu$ around the cathode. Accordingly, the sensitivity of this MET device design is to achieve $10.4\ \mathrm{V/G}$ at 18 Hz. And the sources of noise have been analyzed.

ACKNOWLEDGMENTS

I would like to express my sincere gratitude to my advisor Dr. Hongyu Yu for his support, motivation and immense knowledge on this research project. I would like to thank my committee members: Dr. Junshan Zhang and Dr. Hanqing Jiang for their insightful comments and encouragement.

My sincere thanks also go to my colleague Mengbing Liang and Ruirui Han for all of their help.

Last but not the least, I would like to thank my family for their continuous support and encouragement.

TABLE OF CONTENTS

Page

LIST OF TABLES

LIST OF FIGURES

Figure Page

Figure Page

CHAPTER 1

INTROUCTION

In this chapter, the basic ideas of microelectromechanical systems including its history and development are introduced. Then the working principle of accelerometers, taking capacitive accelerometer as an example, is demonstrated. In addition, the working principles of Molecular Electronic Transducer (MET) and Galvanic cell are introduced and discussed in detail in the last two sections of this chapter.

1.1 Introduction of MEMS

"How many times when you are working on something frustratingly tiny, like your wife's wrist watch, have you said to yourself, "If I could only train an ant to do this!" What I would like to suggest is the possibility of training an ant to train a mite to do this. What are the possibilities of small but movable machines? They may or may not be useful, but they surely would be fun to make."

(From the talk "There's Plenty of Room at the Bottom," by Richard P. Feynman at the annual meeting of the American Physical Society, December 1959.)

Microelectromechanical systems, by definition, is the integration of mechanical elements, sensors actuators and electronics on a common substrate through the utilization of microfabrication technology.[1] It is difficult to determine an exact date when MEMS was introduced since the inception of MEMS devices occurred in many places and through the ideas and endeavors of several individuals. But there is no doubt that new MEMS technologies and applications are being developed every day due to its distinct

advantages. Following is a timeline which includes many endeavors that leading to MEMS development. [2]

- 1948 Invention of the Germanium transistor at Bell Labs (William Shockley)
- 1954 Piezoresistive effect in Germanium and Silicon (C.S. Smith)
- 1958 First integrated circuit (IC) (J.S. Kilby 1958 / Robert Noyce 1959)
- 1959 "There's Plenty of Room at the Bottom" (R. Feynman)
- 1959 First silicon pressure sensor demonstrated (Kulite)
- 1967 Anisotropic deep silicon etching (H.A. Waggener et al.)
- 1968 Resonant Gate Transistor Patented (Surface Micromachining Process) (H. Nathanson, et.al.)
- 1970's Bulk etched silicon wafers used as pressure sensors (Bulk Micromachining Process)
- 1971 The microprocessor is invented
- 1979 HP micromachined ink-jet nozzle
- 1982 "Silicon as a Structural Material," K. Petersen
- 1982 LIGA process (KfK, Germany)
- 1982 Disposable blood pressure transducer (Honeywell)
- 1983 Integrated pressure sensor (Honeywell)
- 1983 "Infinitesimal Machinery," R. Feynman
- 1985 Sensor or Crash sensor (Airbag)
- 1985 The "Buckyball" is discovered
- 1986 The atomic force microscope is invented
- 1986 Silicon wafer bonding (M. Shimbo)
- 1988 Batch fabricated pressure sensors via wafer bonding (Nova Sensor)
- 1988 Rotary electrostatic side drive motors (Fan, Tai, Muller)
- 1991 Polysilicon hinge (Pister, Judy, Burgett, Fearing)
- 1991 The carbon nanotube is discovered
- 1992 Grating light modulator (Solgaard, Sandejas, Bloom)
- 1992 Bulk micromachining (SCREAM process, Cornell)
- 1993 Digital mirror display (Texas Instruments)
- 1993 MCNC creates MUMPS foundry service

- 1993 First surface micromachined accelerometer in high volume production (Analog Devices)
- 1994 Bosch process for Deep Reactive Ion Etching is patented
- 1996 Richard Smalley develops a technique for producing carbon nanotubes of uniform diameter
- 1999 Optical network switch (Lucent)

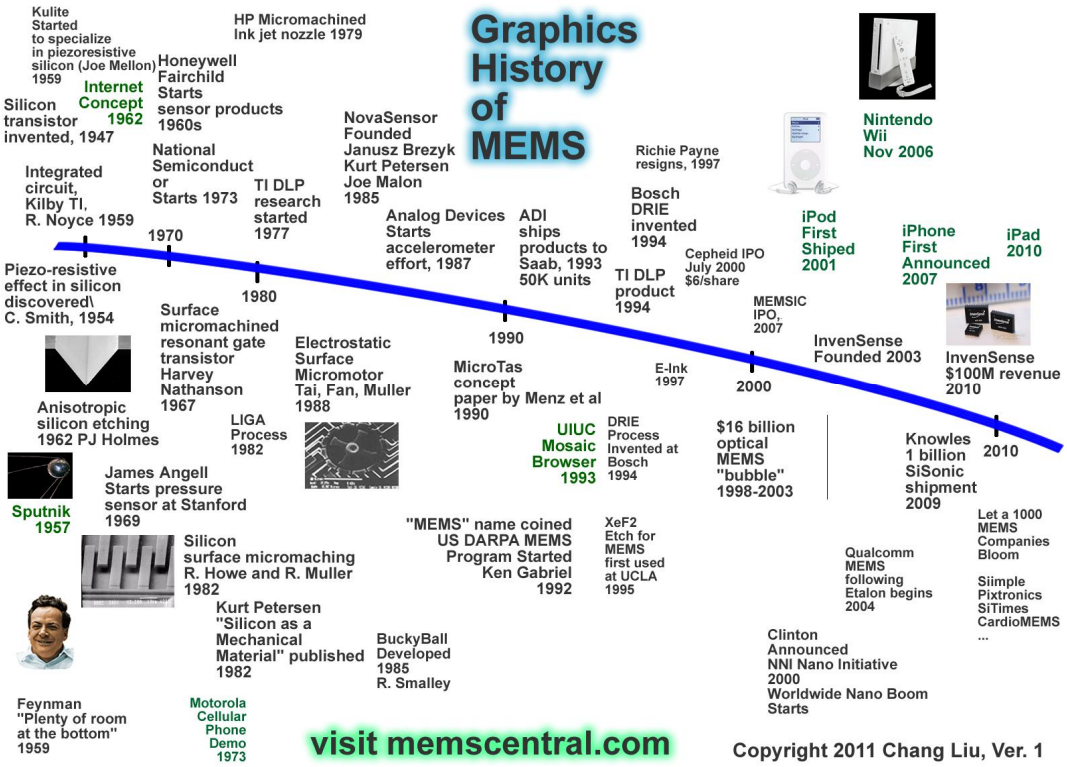

Figure 1. Visual history of MEMS

Why micro-systems? That is because its obvious advantages. Less energy and resources for fabrication means lower cost. Less space occupied, smaller size also means minimally invasive which can be critical in some biological applications. Therefore applications of MEMS have been widely developed in many fields where miniaturization is beneficial, such as: mobile & wearable devices, automotive, aerospace, biomedical, chemical, optical displays, wireless communications and fluidics. Seeing that the MEMS has been widely used in various electronics, it is no surprise that the market for micro-

electromechanical system (MEMS) chips will grow from about $12 billion in 2012 to over $22 billion by 2018, according to market analysts at MEMS Executive Congress 2013.

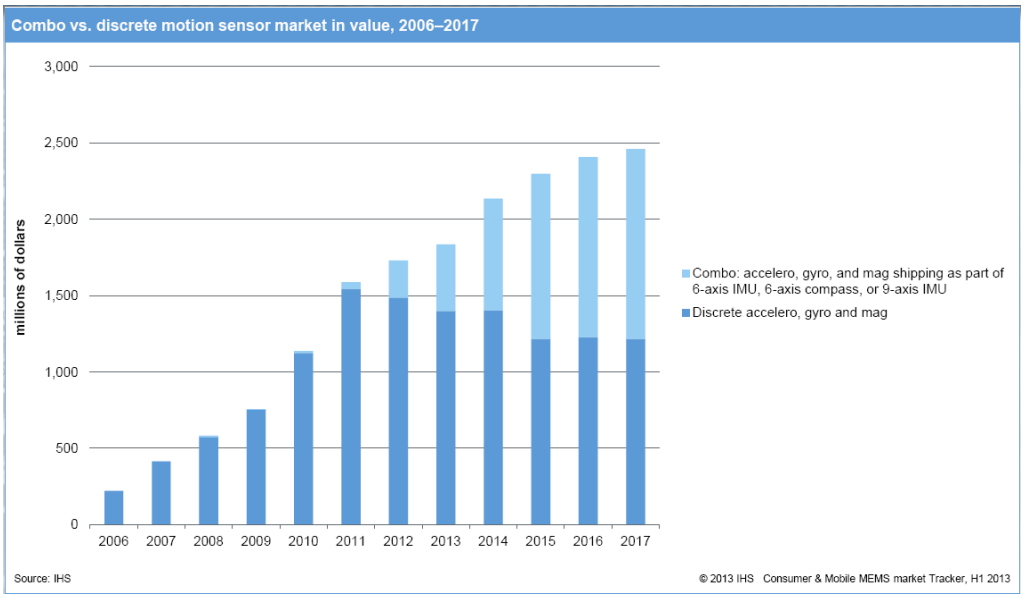

Figure 2. Consumer & Mobile MEMS market Tracker, H1 2013 [3]

1.2 Introduction of Accelerometer

An accelerometer is a device that measures proper acceleration which is the acceleration it experiences relative to freefall. Accelerometers are important in a broad range of disciplines including seismology and resource detection in the oil industry.[4] One way to do motion sensing is to use a solid-state mass-spring system with suspended proof mass, creating a damped simple harmonic oscillator with motion. When the accelerometer experiences an acceleration, the proof mass is displaced to the point that the spring is able to give the mass the same acceleration as the frame. The displacement is then measured to calculate the acceleration.

Piezoelectric, piezoresistive and capacitive components are the three most widely used to convert the mechanical motion into an electrical signal. Piezoelectric accelerometers rely on piezoceramics or single crystals. They are superior in upper frequency range and high temperature range. While piezoresistive accelerometers measure acceleration by the change in resistance due to stress in suspended beam and they generally less sensitive than capacitive accelerometers.[5] Typically capacitive accelerometers is superior in the low frequency range and they can be operated in servo mode to achieve high stability and linearity.

In a capacitive accelerometer, differential capacitors are used to sense the relative movement of the proof-mass to the reference frame. As shown in Figure 3,[5] there are three electrodes used for the measurement. Vo is the output, two capacitors C_1 and C_2 show equal capacitance value when the moveable component is centered. Motion of the moveable component would increases one capacitance and decreases the other. If the gap of the upper capacitor is G_1 and that of the lower capacitor is G_2, and areas of both capacitors are the same. If a voltage of +Vs is applied to the upper plate, and a voltage of –Vs is applied to the lower plate simultaneously. The output voltage Vo is

$$V_o = -V_S + \frac{C_1}{C_1 + C_2}(2V_S) = \frac{C_1 - C_2}{C_1 + C_2}V_S \quad (1)$$

As the areas of C_1 and C_2 are equal, the output voltage Vo is

$$V_o = \frac{G_2 - G_1}{G_1 + G_2}V_S \quad (2)$$

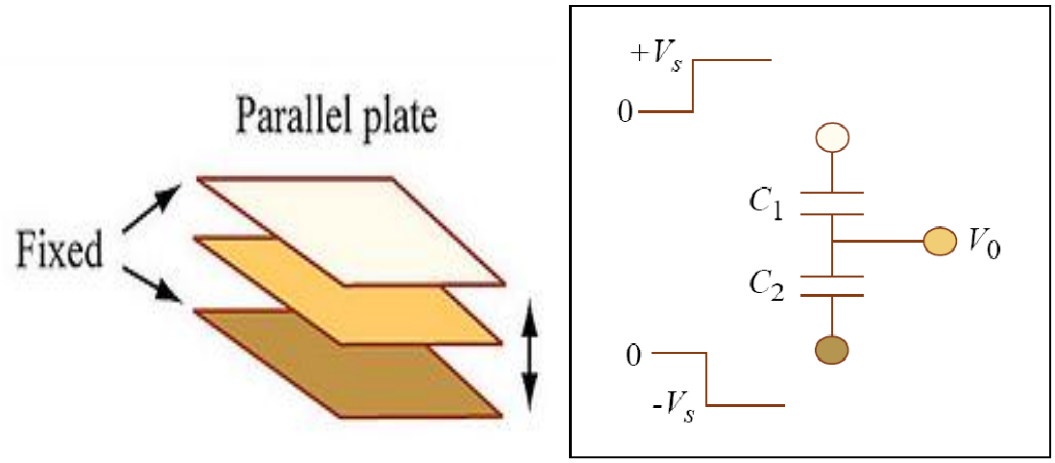

Figure 3. Schematic of differential capacitors and circuit model

While the performance of solid state MEMS accelerometers is not satisfactory, this is due to the increase of resonant frequency with decreasing proof mass during miniaturization. Molecular electronic transducers provides an alternative paradigm for low frequency acceleration measurement.

1.3 Operation Principle of Molecular Electronic Transducer

Molecular electronic transducers (MET) are a class of inertial sensors (including accelerometers, gyroscopes, tilt sensors, seismometers) based on an electrochemical mechanism. In MET devices, the physical and chemical phenomena that occur at the surface of electrodes in electrochemical cells are captured as the result of hydrodynamic motion. MET is a kind of electrolytic cell designed so that motion of the device, which causes a movement in the liquid electrolyte, can be converted to an electronic signal proportional to acceleration or velocity of MET.

Compared to the solid-state accelerometer, MET transducer use a liquid-state inertial mass. Therefore there is no moving solid mechanical parts vulnerable to possible damage in MET accelerometers and making them able to withstand high shock. In

addition, MET accelerometers possess high sensitivity and low self-noise in low frequency range with appropriate parameters. As shown in Figure 4, the electrochemical cell in MET accelerometer consist of sensing channels. Each of these channels has four electrodes separated by dielectric spacers and highly flexible rubber diaphragm. Concentrated I_2/I^- electrolyte is filled into the channels working as inertial proof mass.

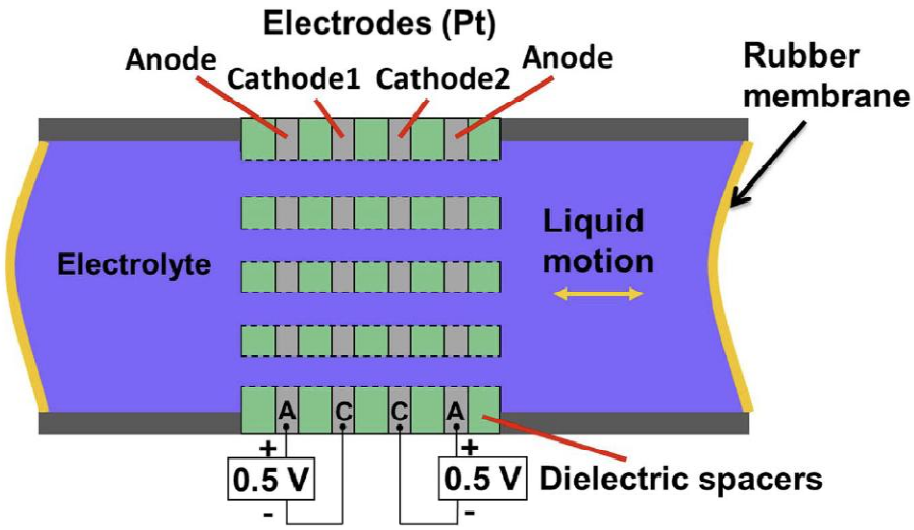

Figure 4. Schematic of a traditional MET accelerometer using standard machined platinum mesh separated by dielectric grids as sensing cell.

The working principle of the traditional MET accelerometer is a reversible redox reaction which does not involving either plating of a metal or release of a gas. The redox reaction is:

$$3I^- \rightarrow I_3^- + 2e^- \quad anode\ reaction$$

$$I_3^- + 2e^- \rightarrow 3I^- \quad cathode\ reaction$$

These anode and cathode reaction occur in a continuous fashion when a voltage between 0.2 to 0.9 volt applied across electrodes. As the reactions going on, most of the I_3^- are around the anode creating a concentration gradient of I_3^- between electrodes. when

the cell is stationary, the current stays at a low steady-state value. While any motion of the cell will cause convection in the electrolyte and thus change the concentration gradient of I_3^- and bring more I_3^- to the cathode. Therefore result in an increase of current proportional to the motion.

However, there are several disadvantages for the traditional MET accelerometer including high cost of fabrication, restricted possibility to optimize performance, high scatter of parameters due to manual production of transducers and poor compatibility to CMOS manufacturing. [6] These disadvantages motivated the development of new MET accelerometer with low cost, high sensitivity and reproducibility.

1.4 Operation Principle of Galvanic Cell

A galvanic cell is an electrochemical cell that derives electrical energy from spontaneous redox reactions taking place within the cell. It generally consists of two different metals connected by a salt bridge, or individual half-cells separated by a porous membrane.

In electrochemistry, salt bridge is a laboratory device used to connect the oxidation and reduction half-cells of a galvanic cell (voltaic cell), a type of electrochemical cell. It maintains electrical neutrality within the internal circuit, preventing the cell rapidly running its reaction to equilibrium. If no salt bridge were present, the solution in one half cell would accumulate negative charge and the solution in other half cell would accumulate positive charge as the reaction proceeded, quickly preventing further reaction, and hence production of electricity.

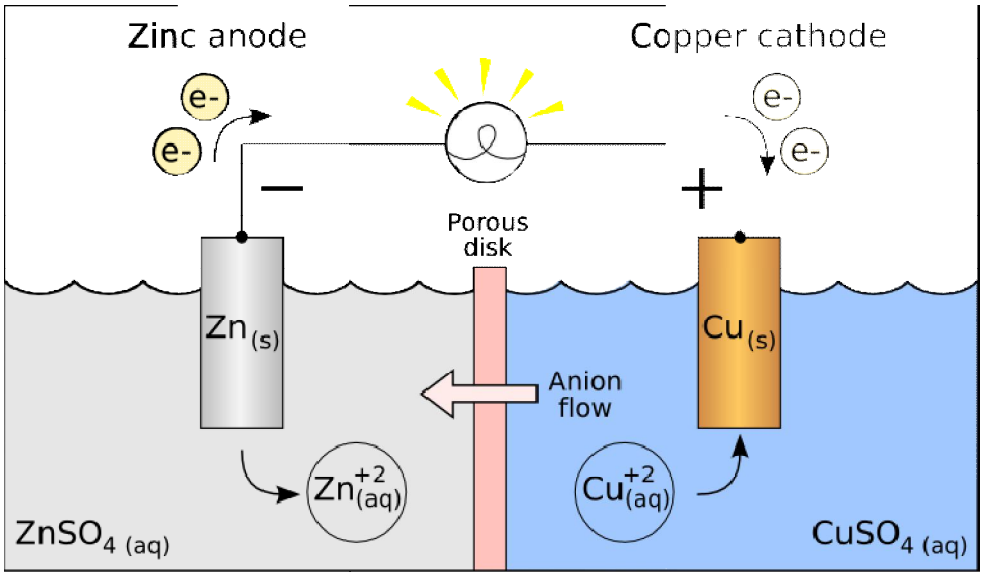

Figure 5. Galvanic cell with no cation flow.

A galvanic cell can be regarded as a combination of two half-cells. Each half-cell consists of a solid metal (electrode) which is submerged in a solution. The solution contains cations of the electrode metal and anions to balance the charge of the cations. Inside each half-cell, there is a redox reaction that is in chemical equilibrium, which can be written as follows:

M^{n+} (oxidized species) + $ne^{-} \leftrightarrow$M (reduced species)

In which M^{n+} represents a metal cation, an atom that has a charge imbalance due to the loss of electrons, M represents a metal.

A galvanic cell consists of two half-cells, one electrode is composed of metal A, and the other electrode is composed of metal B. Then the redox reactions for the two separate half-cells are:

$A^{n+} + ne^{-} \leftrightarrow A$

$B^{m+} + me^{-} \leftrightarrow B$

then, combining these two reactions, these two metals can react with each other:

$$m\ A + n\ B^{m+} \leftrightarrow n\ B + m\ A^{n+}$$

That is to say, the metal atoms of one half-cell can reduce the metal cations of the other half-cell or conversely, the metal cations of one half-cell can oxidize the metal atoms of the other half-cell. This all depends on the electronegativity of the two metals. When metal B possesses a greater electronegativity than metal A, then metal B tends to grab electrons from metal A (i.e. metal B tends to oxidize metal A), thus one direction of the reaction is favored over the other:

$$m\ A + n\ B^{m+} \rightarrow n\ B + m\ A^{n+}$$

A metal wire connecting the electrodes is necessary to conduct the electrons that participate in the reaction. In one half-cell, dissolved metal-B cations combine with the free electrons that are available at the interface between the solution and the metal-B electrode; these cations are thereby neutralized, causing them to precipitate from solution, this process is also called plating.

The reduction reaction causes the free electrons throughout the metal-B electrode, the wire, and the metal-A electrode to be pulled into the metal-B electrode. Consequently, electrons are wrestled away from some of the atoms of the metal-A electrode, as though the metal-B cations were reacting directly with them; those metal-A atoms become cations that dissolve into the surrounding solution.

As contrary to the reduction reaction, the half-cell with the metal-A electrode develops a positively charged solution (due to the dissolution of metal-A cations into it), while the other half-cell develops a negatively charged solution (as the metal-B cations

precipitate out of the solution leaving behind the anions). This imbalance in charge will obviously stop the reaction.

So a salt bridge is needed to keep charge balanced. The solutions are connected by a salt bridge or a porous plate in order to conduct the ions (both the cations from one solution and the anions from the other solution), which balances the charges of the solutions and thereby allows the reaction between metal A and metal B to continue without interuption.

There are several conventions relating to cell notation and nomenclature:

- The anode is where oxidation reaction occurs, and the cathode is the site where reduction reaction occurs. In an galvanic cell, the identity of the electrodes depends on the actual direction in which the net cell reaction is occurring.
- If electrons flow from the left electrode to the right electrode (as depicted in the above cell notation) when the cell operates in its spontaneous direction, the potential of the right electrode will be higher than that of the left, and the cell potential will be positive.
- "Conventional current flow" is from positive to negative, which is opposite to the direction of the electron flow. This means that if the electrons are flowing from the left electrode to the right, a galvanometer placed in the external circuit would indicate a current flow from right to left.

For the Galvanic cell depicted in the figure, the anode is zinc and the cathode is copper, and the anions in the solutions are sulfates (SO_4^{2-}) of the respective metals. When an electrically conducting device (e.g. metal wire) connects the electrodes, the electrochemical reaction is:

$Zn + Cu^{2+} \rightarrow Zn^{2+} + Cu$

The zinc electrode is dissolved and copper is deposited on the copper electrode. Such losing and receiving electrons process takes place within a very thin interfacial region at the electrode surface through quantum mechanical tunneling of electrons between the electrode and the electroactive species. In the previous example of Zn/Cu galvanic cell, the electrode reaction involves a metal and its hydrated cation, which is called metal-metal ion electrodes. And the work required for displacing the water molecules in the hydration spheres of the ions is part of the activation energy of this process.

CHAPTER 2

FABRICATION PROCESS

MEMS fabrication shares many of the same standard technologies with the integrated circuit (IC) domain (e.g. photolithography, etching, oxidation, diffusion, ion implantation, sputtering, chemical vapor deposition, etc.) And MEMS combines these capabilities with specialized micromaching process for MEMS fabrication. Before 1996, almost all MEMS processes fall into two primary types: bulk micromachining and surface micromachining. [7] Bulk micromachining is most widely known commercially in production of membranes for pressure sensors and nozzles for inkjet printing. While surface micromachining processes create microstructures out of thin film on the substrate surface. Commercial examples of surface micromachining includes projection arrays and airbag accelerometers. Contrast to solid-state electronics, METs characterized by charge transfer via ions in solution. Solion, a term derived from the words solution and ions, was first developed in the 1950s and developed by US-Navy and others up through the 1970s. Work on Solion motion sensors including physical and mathematical studies of the underlying electrochemical and fluid flow dynamics was continued primarily in Russia, where the term “Molecular Electronic Transducers” was used to describe such devices. The advantages of MET motion sensors include their small size, lack of fragile solid-state moving parts, high sensitivity and low noise floor at low frequencies, and the response independent of installation angle.[8]

2.1 Typical Process for MEMS

Bulk micromachining is regarded as the oldest MEMS technology. This technique includes the selective removal of the substrate material to create miniaturized mechanical components. Bulk micromachining can be accomplished via chemical or physical means, with chemical means being far more popular in the MEMS industry. [9]

Chemical wet etching is a widely used bulk micromachining technique, which will etch exposed regions of the substrate at measurable rates by immersing a substrate into a solution of reactive chemical. Chemical wet etching is popular in MEMS because of its very high etching rate and selectivity. Furthermore, the etching rate and selectivity are tunable, they can be modified in several ways: altering the chemical composition of the etching solution, adjusting temperature of the etching solution; modifying the dopant concentration in the substrate; and choosing which crystallographic planes of the substrate are exposed to the etching solution.

There are two types of chemical wet etching in bulk micromachining: isotropic wet etching and anisotropic wet etching. In isotropic wet etching, the etch rate is independent of the crystallographic orientation of the substrate and the etching rates in all directions are the same. As stirring can make a big difference in practice lateral etching, isotropic wet etching is almost always performed with vigorous stirring of the etching solution. Figure 1 illustrates the profile of the etch using an isotopic wet etchant with and without stirring of the etchant solution.

During etching process, a masking material is required, with a high selectivity relative to the substrate material. Silicon dioxide and silicon nitride are two widely used

masking materials for isotropic wet silicon etching. Silicon nitride possesses a much lower etching rate compared to silicon dioxide and therefore is more frequently used.

The much more widely used wet etching micromachining are anisotropic wet etching. Anisotropic wet etching works by immersing the substrate into a chemical solution where the etch rate is dependent on crystallographic orientation of the substrate. The etching rates vary according to silicon crystal planes is attributed to the different bond configurations and atomic density at the different planes exposed to the etchant solution. Wet anisotropic etching is usually described in terms of etch rates according to the different normal crystallographic places, usually <100>, <110>, and <111>. In general, silicon anisotropic etching is slower along the <111> planes than all the other planes in the lattice and the difference between the different lattice directions in etch rate can be up to 1000:1. It is believed that the reason for the slower etch rate on the <111> planes is that these planes have the highest density of exposed silicon atoms in the etching solution, as well as 3 silicon bonds below the plane, thereby leading to somewhat chemical shielding of the surface.

Figure 6 below is an illustration of the shapes that created by anisotropic wet etching of <100> oriented silicon substrates (an inverted pyramidal and a flat bottomed trapezoidal etch pit). Note that the shape of the etch pattern is primarily determined by the slower etching <111> planes.

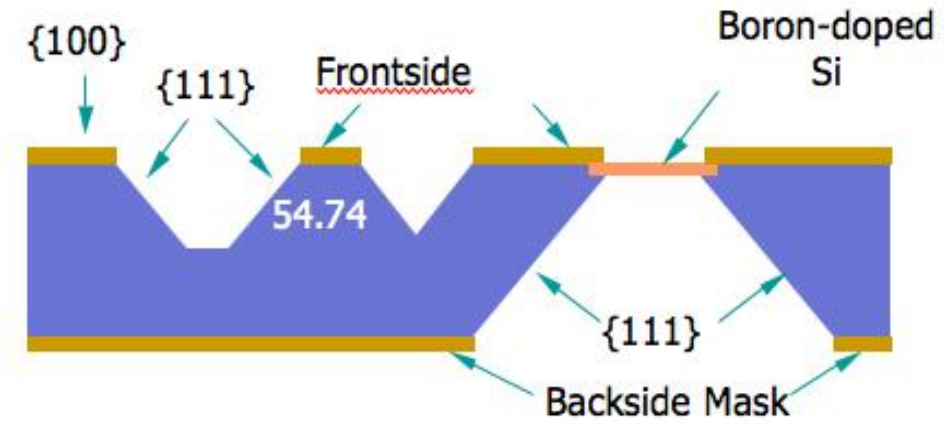

Figure 6. Illustration of the etch profiles of a <100> oriented silicon substrate after immersion in an anisotropic wet etching solution.

Another very popular technology for the fabrication of MEMS devices is surface micromachining. Depending on the materials and etchant that are used, there are many variations of how surface micromachining is performed. However, this process usually starts with the deposition of a thin-film to act as a mechanical base onto which the actual device layers are built. Subsequently the deposition and patterning of another layer of thin-film which is referred to as the structural layer. Then removal of the base layer to release the mechanical structure layer from the constraint of the underlying layer, thus allowing the structural layer to move. An illustration of a surface micromachining process is shown in Figure 7. In this example, an oxide layer is first deposited and patterned. This oxide layer is temporary and referred to as the sacrificial layer. Then a thin layer of polysilicon is deposited and patterned and this layer is the structural mechanical layer. At last, the sacrificial layer is removed and the polysilicon layer is free to move as a cantilever.

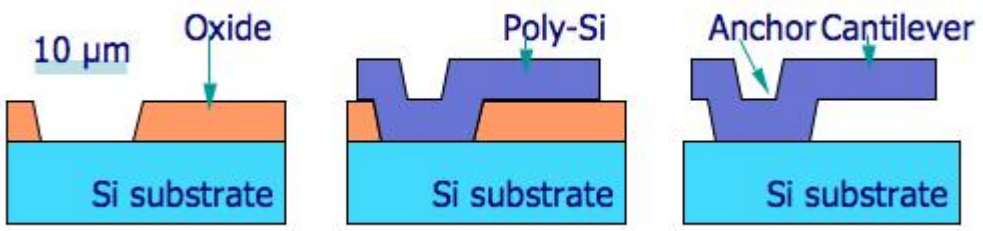

Figure 7: Illustration of a surface micromachining process.

One of the reasons surface micromachining is so popular is that it provides precise dimensional control in the vertical direction. This can be attributed to the fact that the thicknesses of structural and sacrificial layer are defined by deposition which can be accurately controlled. In addition, surface micromachining provides precise dimensional control in the horizontal direction, as the structural layer tolerance is defined by the fidelity of the photolithography and etch processes used. Other advantages of surface micromachining include: a large variety of combinations of structure, sacrificial and etchant can be used; some are compatible with microelectronics devices to enable integrated MEMS devices. Surface micromachining frequently exploits the thin-film deposition characteristics such as conformal coverage with LPCVD. Lastly, surface micromachining uses single-sided wafer processing and is relatively simple. This allows higher integration density and lower cost per die compared to bulk micromachining.

Deep reactive ion etching (DRIE) is one of the most widely used processes in MEMS community. Deep reactive ion etching is usually used to create structures with very high aspect ratio with a depth of the etch can be even thousands of microns into substrate. There are two main methods for deep reactive ion etching: cryogenic and Bosch. While Bosch technology is the one recognized for production. Figure 8 illustrates

how deep reactive ion etching is accomplished. Basically it is a process of alternatively etch the silicon with high density plasma and deposit a layer of etch resistant polymer on the sidewalls. Sulfur hexafluoride (SF_6) is often used for silicon etching and octafluorocyclobutane (C_4F_8) gas is commonly used to produce a protective layer similar to Teflon. As shown in following figure, the sidewall created with DRIE is not perfect but is characterized with washboard pattern.

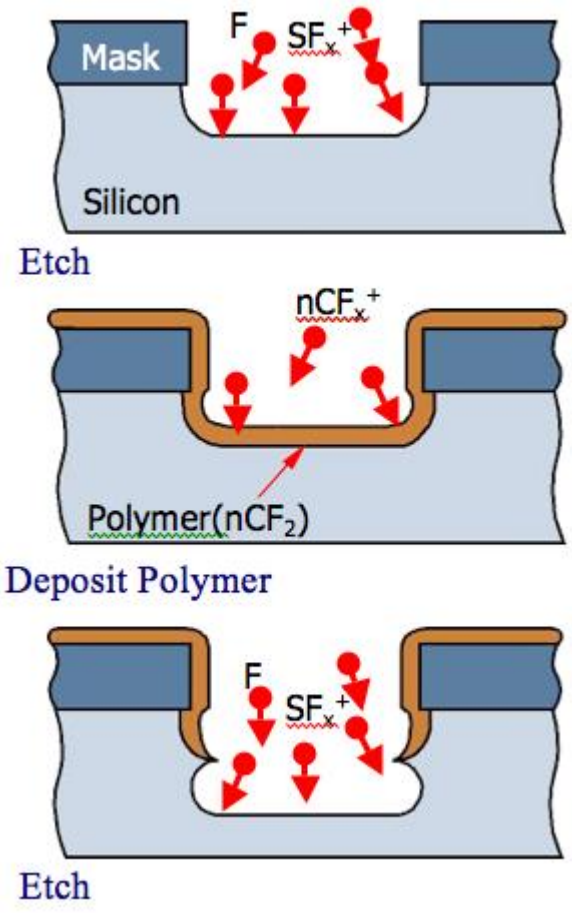

Figure 8. Illustration of how deep reactive ion etching works.

Besides wet and dry etching, lift-off is another way to pattern metal or dielectric thin films. Lift-off process create structures on a target material on the surface of a substrate by using a sacrificial material (usually photoresist).

First, a sacrificial stencil layer is deposited on the surface of the substrate, then an inverse pattern is created on it as shown in Figure 9. This is done by etching openings through the sacrificial layer so that the target material can reach the substrate in those regions (pink part in Figure 9. (b)). Different from common etching process which using the resist as covering layer, target material deposition is provided after the photolithography process in lift-off. The target material is then deposited over the whole area, reaching the surface of the substrate in the etched regions (pink part in Figure 9. (b)) and staying on the top of the sacrificial layer in the regions (blue part in Figure 9. (b)). After the deposition, the sacrificial layer is washed away. Thus the material on the top (blue part in Figure 9. (b)) is washed off together with the sacrificial layer below. After the lift-off, the target material remains only in the regions where it had a direct contact with the substrate. Note that different patterns are needed with different photoresist, positive or negative.

With respect to patterning, various methods , such as extreme ultraviolet lithography or electron beam lithography, can be used according to the photoresist type.

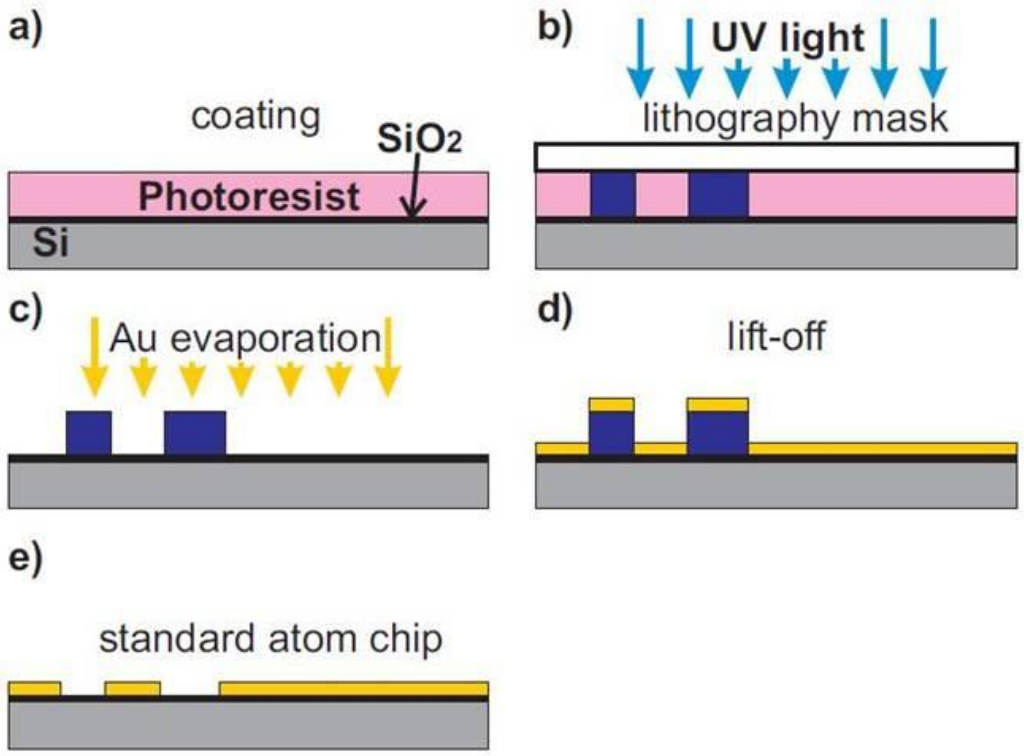

Figure 9. Schematic of lift-off process.

Target material (usually a thin metal layer) is deposited (on the whole surface of the wafer). This layer covers the remaining resist as well as parts of the wafer that were cleaned of the resist in the previous developing step.

The rest of the sacrificial material (ex. photoresist) is washed out together with parts of the target material covering it, only the material that was in the "holes" having direct contact with the underlying layer (substrate/wafer) stays

2.2. Improved Fabrication Process for Molecular Electronic Transducer

It has been found that the noise of the micro MET seismometer is heavily depends on the hydrodynamic resistance in the MET device. And the hydrodynamic resistance of a channel is inversely proportional to the 4^{th} order of the radius of the channel cross-

section and the number of parallel channels, and proportional to the length of the channel. [8] However, attempts to improve the noise performance of the MET based seismometer by increase in number of channels and radius of the channel cross-section have limited by the fabrication technique, i.e. FIB process and the thin diaphragm. First, FIB milling, which can only process one device at a time, is a very time consuming and costly process. So the cost of the MET based seismometer will increase with improving noise performance. Second, the quality of the FIB milling will decrease when the number of channels is too big to clean all of them. Also, either increase in number of channels or radius of the channel cross-section can make the diaphragm more vulnerable to breakage. Therefore these changes could lower the yield of the device. To overcome the above limitations, two alternative fabrication processes based on SOI (silicon on insulator) wafers have been developed. [8]

Silicon on insulator (SOI) refers to the technology that using a layered silicon–insulator–silicon substrate to replace conventional silicon substrates in semiconductor manufacturing. Such replacement in SOI technology can reduce parasitic device capacitance and thereby improve device performance. In SOI-based devices, the junction is on top of an electrical insulator, typically silicon dioxide or sapphire instead of silicon. The choice of insulator depends on potential application. Sapphire is used as the insulator for high-performance radio frequency (RF) and radiation-sensitive applications, and silicon dioxide is used for diminished short channel effects in microelectronics devices. [10]

2.2.1 Single-SOI Fabrication Process

Single-SOI fabrication process starts with a SOI wafer with a thick device layer (150 µm) and box layer (5 µm) as substrate. First, AZ4620 photoresist is patterned on the backside of the SOI wafer, working as mask for deep reactive ion etching (DRIE) on silicon handle layer to form part of the channel.[8] DRIE process stops when the remaining thickness of the handle layer equal to that of the device layer to ensure the symmetry of the electrodes. Then, the top silicon device layer is patterned into circles of 200 µm in diameters with AZ4620. Afterward, DRIE is performed on the top silicon device layer until reaching the box layer (SiO_2) of the SOI wafer. Then the remained photoresist along with the silicon will act as mask for wet etching of the box layer -SiO_2. Here the undercut of the SiO_2 is desired for the subsequent isolation between electrodes. Then, the remaining silicon will be etched by DRIE until the entire channels are open. Photoresist is then removed and electrode (Ti/Pt) will be deposited onto the top and bottom surface of silicon and also the sidewall of channel by E-beam deposition. By choosing a appropriate angle between the metal source and the target wafer, there would be no metal deposition on the sidewall of SiO_2 recess. Finally, two of the above fabricated wafers are selectively coated with a layer of Parylene-C and then bonded to form the sensing element with four isolated electrodes.

Therefore, there could be a significant increase in the strength of supporting structure with this fabrication process. So the diameter of the channels can go up to 200 µm and the number of channels can go up to 800. Meanwhile, since no FIB processes involved, the devices can be fabricated in batch. This can greatly save the fabrication cost and time. However, the trade-off is the rougher sidewall surfaces and imperfect alignment.

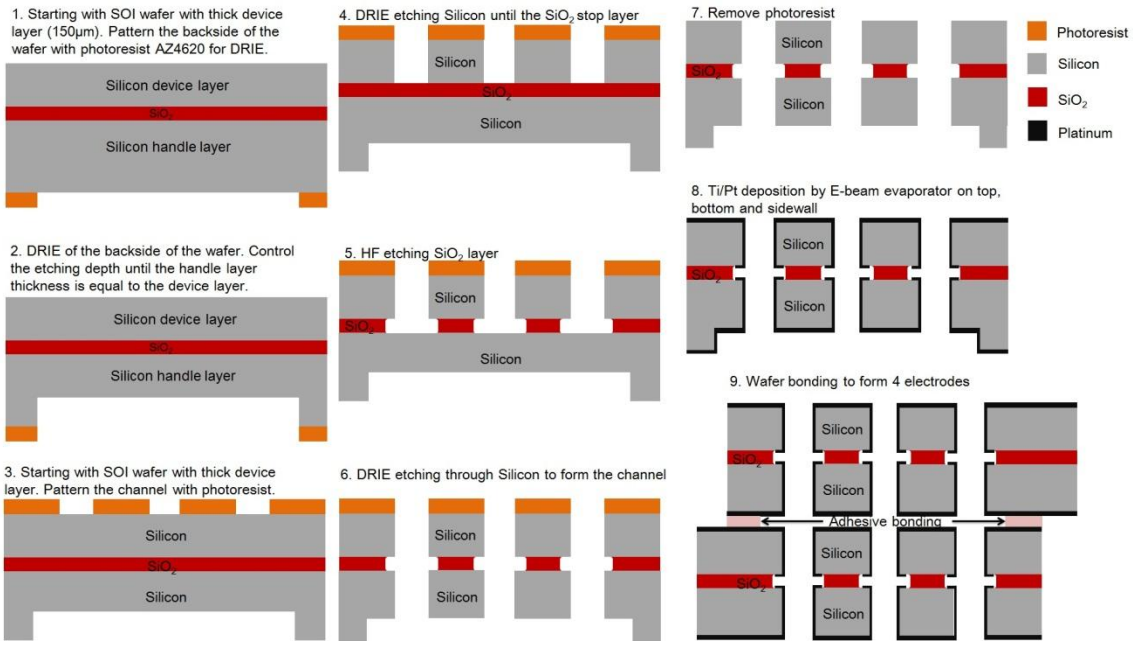

Figure 10. Fabrication processes of the sensing element of MET based micro seismometer with single- SOI wafers.

With this SOI method, the hydrodynamic resistance R_h, which is a indicator of the device noise performance, of a multiple channel device can be four orders of magnitude lower than a single channel device developed in regular design. So the self-noise of the device by SOI method is expected to be much lower.

2.3. 3D printing

3D printing or additive manufacturing is any of various processes used to synthesize a three-dimensional solid object from a digital file. The very first 3D printing technology became visible in late 1980's. In 1986, the first patent for stereolighography apparatus was issued to Charles Hull, [11] the co-founder of 3D Systems Corporation.

There are several different 3D printing processes according to the way layers are deposited to create parts and also the materials that are used. Table 1 shows different methods used for 3D printing.

Table 1 Different methods used for 3D printing.

Type	Technologies	Materials
Extrusion	Fused deposition modeling (FDM) or Fused Filament Fabrication (FFF)	Thermoplastics, eutectic metals, edible materials, Rubbers, Modeling clay, Plasticine, Metal clay (including Precious Metal Clay)
	Robocasting or Direct Ink Writing (DIW)	Ceramic materials, Metal alloy, cermet, metal matrix composite, ceramic matrix composite
Light polymerized	Stereolithography (SLA)	photopolymer
	Digital Light Processing (DLP)	photopolymer
Powder Bed	Powder bed and inkjet head 3D printing (3DP)	Almost any metal alloy, powdered polymers, Plaster
	Electron-beam melting (EBM)	Almost any metal alloy including Titanium alloys
	Selective laser melting (SLM)	Titanium alloys, Cobalt Chrome alloys, Stainless Steel, Aluminium
	Selective heat sintering (SHS)	Thermoplastic powder
	Selective laser sintering (SLS)	Thermoplastics, metal powders, ceramic powders
	Direct metal laser sintering (DMLS)	Almost any metal alloy
Laminated	Laminated object manufacturing (LOM)	Paper, metal foil, plastic film
Wire	Electron beam freeform fabrication (EBF)	Almost any metal alloy

As shown in Table 1, for selective laser melting (SLM) or direct metal laser sintering (DMLS), selective laser sintering (SLS), fused deposition modeling (FDM) the material needs to be melt or soften before it can be used to produce the layers, while others methods using different sophisticated technologies, such as stereolithography (SLA). For laminated object manufacturing (LOM), thin layers are cut to shape and then joined together. Each method has its own advantages and disadvantages. For example

FDM is considered to be simple and environment-friendly, but this technology is somewhat restricted in the variation of shapes that may be fabricated, therefore it usually cannot produce stalactite-like structures. Selective laser sintering is more popular among manufacturers rather than amateurs since it is very expensive due to the requirement of high-powered lasers. Laminated object manufacturing is one of the most affordable and fastest method for 3D printing.

Stereolithography (SLA) is the oldest one in the history of 3D printing as it was patented as a method of rapid prototyping in 1986 by Charles Hull. Instead of extruding ink or some other liquid onto a surface, SLA machine starts with excess of liquid plastic (photopolymer) and then harden the liquid plastic layer by layer with ultraviolet laser to conduct 3D printing. SLAs have four main parts: a tank that can be filled with liquid plastic (photopolymer), a platform that is lowered into the tank, ultraviolet laser and a computer that controls the platform and the laser.

The length of time that stereolithography takes to produce a part depends on the size and complexity of the part. [12] And speed is one of the advantages of stereolithography. But cost would be a concern of SLA technique as expensive photopolymers are required and SLA machine itself is expensive also.

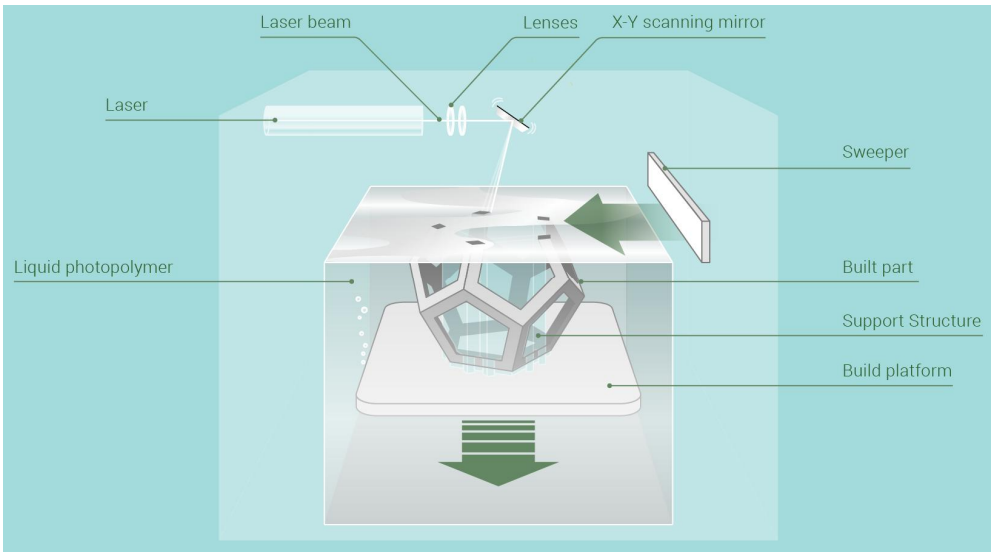

Figure 11. Schematic of Stereolithography 3D printing

In this work, Form 1+ 3D printer from Formlabs is used to create the electrochemical cell for prototype test. The electrochemical cell is sealed with high flexible diaphragms (silicone rubber) at portholes.

CHAPTER 3

EXPERIMENTAL RESULTS

3.1 Experimental Setup

Schematic experimental setup is shown in the Figure 12, data collecting part is isolated from the vibration area in order to cut out distraction. With Data Acquisition Card, vibration data can be recorded by the Labview and sensitivity and resolution of the MET sensor can be calculated according to the time domain chart with fast Fourier transform (FFT) tool.

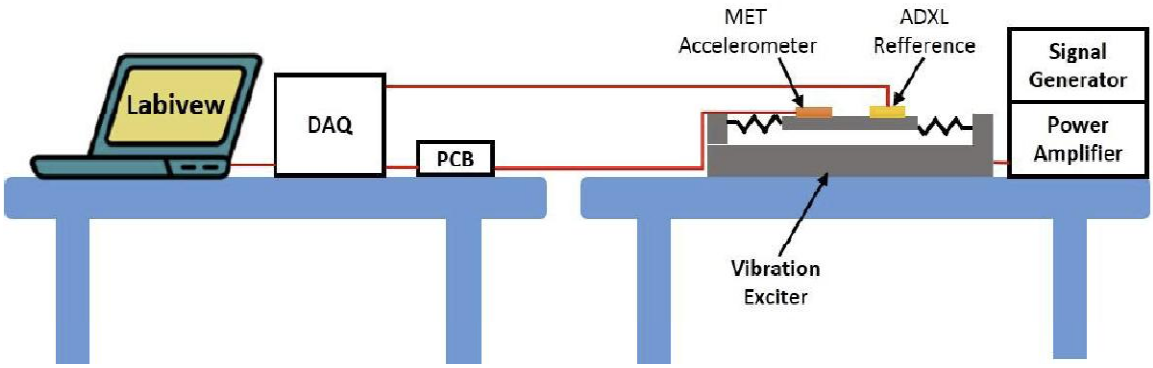

Figure 12. Schematic experimental setup.

The MET accelerometer cell is created by 3D printing (Form 1+ SLA 3D printer from Formlabs) with photopolymer. Figure 13 shows the MET accelerometer cell. The cell is 32 mm long, 24 mm wide. Two rectangular openings on the top are for inserting electrodes. The copper and zinc electrodes are both 11 mm wide, 17.5 mm long and 1mm thick. And holes of 1 mm in diameter are drilled on electrodes to allow the motion of electrolyte in the cell. Between the two electrodes is a 2 mm thick dielectric polymer sheet to keep two electrodes away. The polymer sheet is also drilled at the same positions

as the electrodes. After mounting electrodes, the gap between electrodes and the cell is sealed with Epoxy to ensure no leakage.

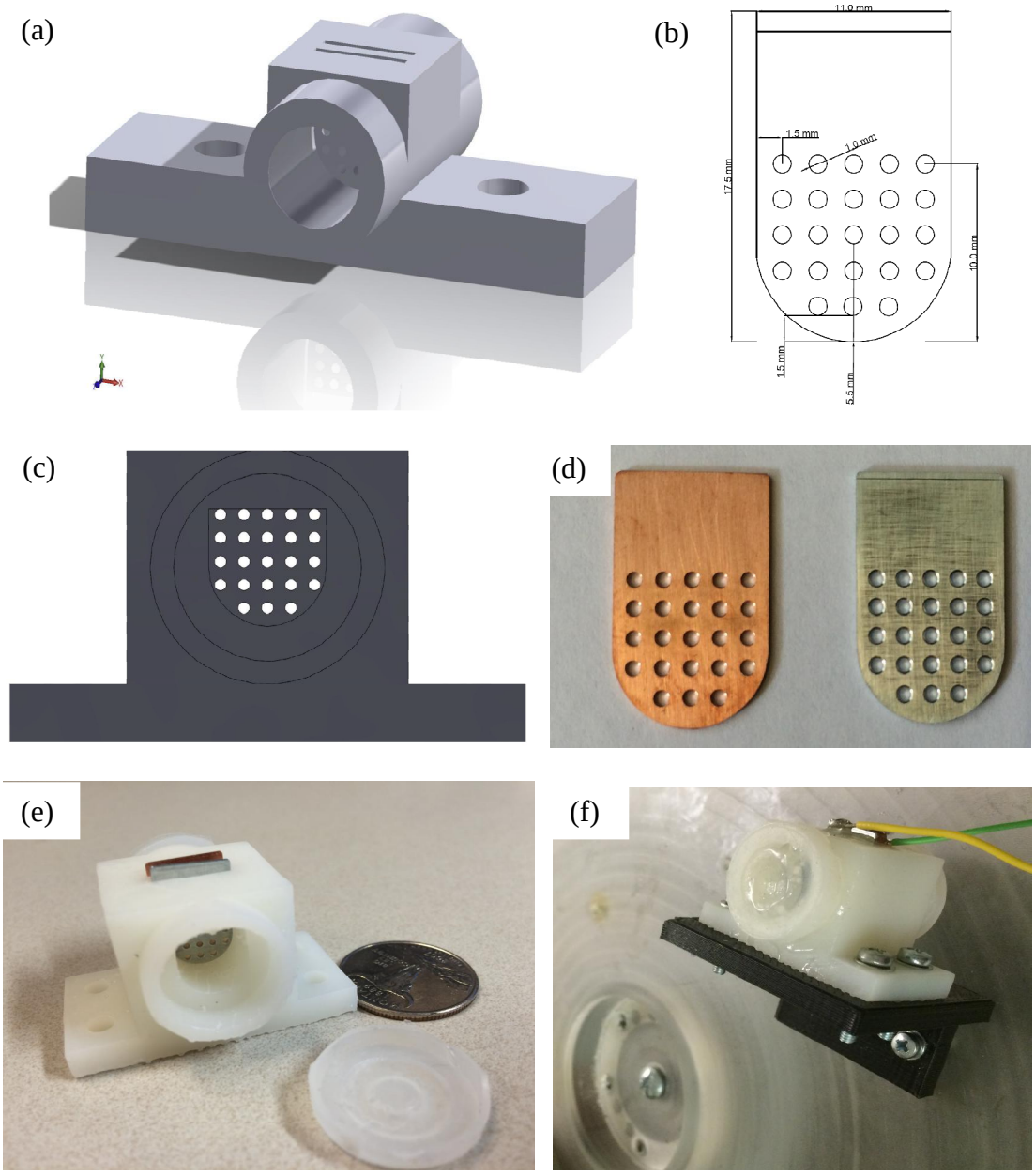

Figure 13. Schematic of MET accelerometer cell (a), Schematic of Zn/Cu electrode (b), Cross section of MET accelerometer cell (c), Zn/Cu electrode (d), MET accelerometer cell printed by Form 1+ 3D printer and silicone cap (e), MET accelerometer cell filled with saturated CuI solution mounted on vibration generator (f).

The MET accelerometer cell is sealed with high flexible silicone rubber on both portholes and is filled with saturated CuI solution.

As a differential amplifier, instrumentation amplifier has a very low DC offset. As MEMS sensors work with low power supply, instrumentation amplifier, possessing low input referred noise and high open-loop gain, is a satisfactory solution . AD620 instrumentation amplifier is used to amplify output signals. AD620 is a low cost, high accuracy instrumentation amplifier capable of high gain with only one external resistor.

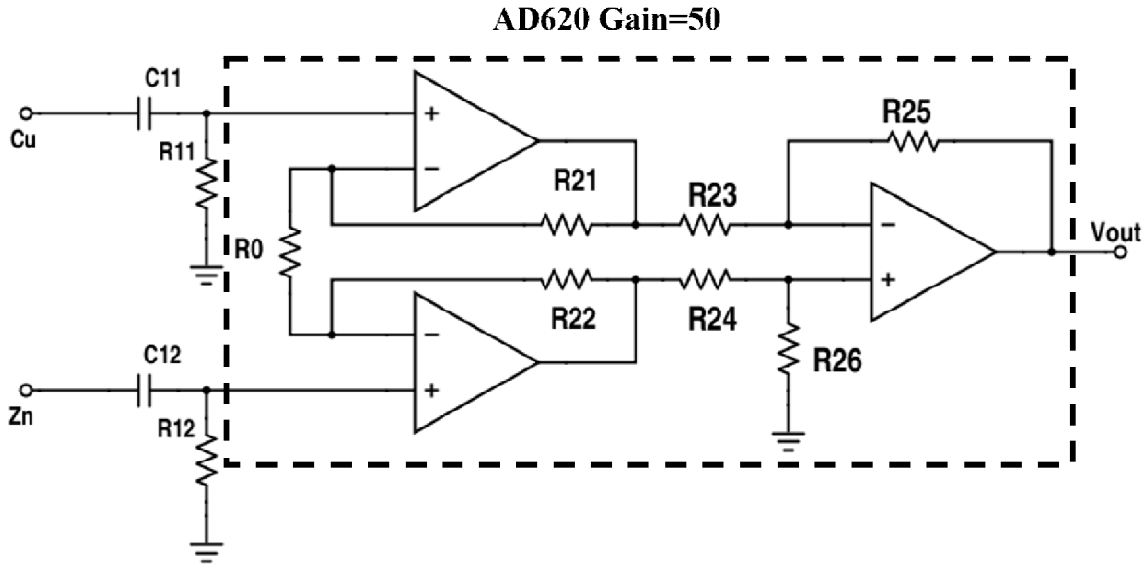

Figure 14. Structure of instrumentation amplifier

Capacitors are used to connect Zn/Cu electrodes and instrumentation amplifier to filter out DC current.

3.2. Experimental Results

PCB 393B31 piezoelectric accelerometer is used as an acceleration reference with frequency range 0.1 to 200 Hz. PCB 393B31 piezoelectric accelerometer is a easy to use accelerometer with low noise at 0.01 $\mu g/\sqrt{Hz}$ level at 10Hz. Figure 15 shows a Comparison of voltage output of PCB 393B31 piezoelectric accelerometer and MET accelerometer, which are both mounted on the vibration generator. Both outputs of PCB 393B31 and MET accelerometer are sinusoidal as the input signal of the vibration generator is sinusoidal.

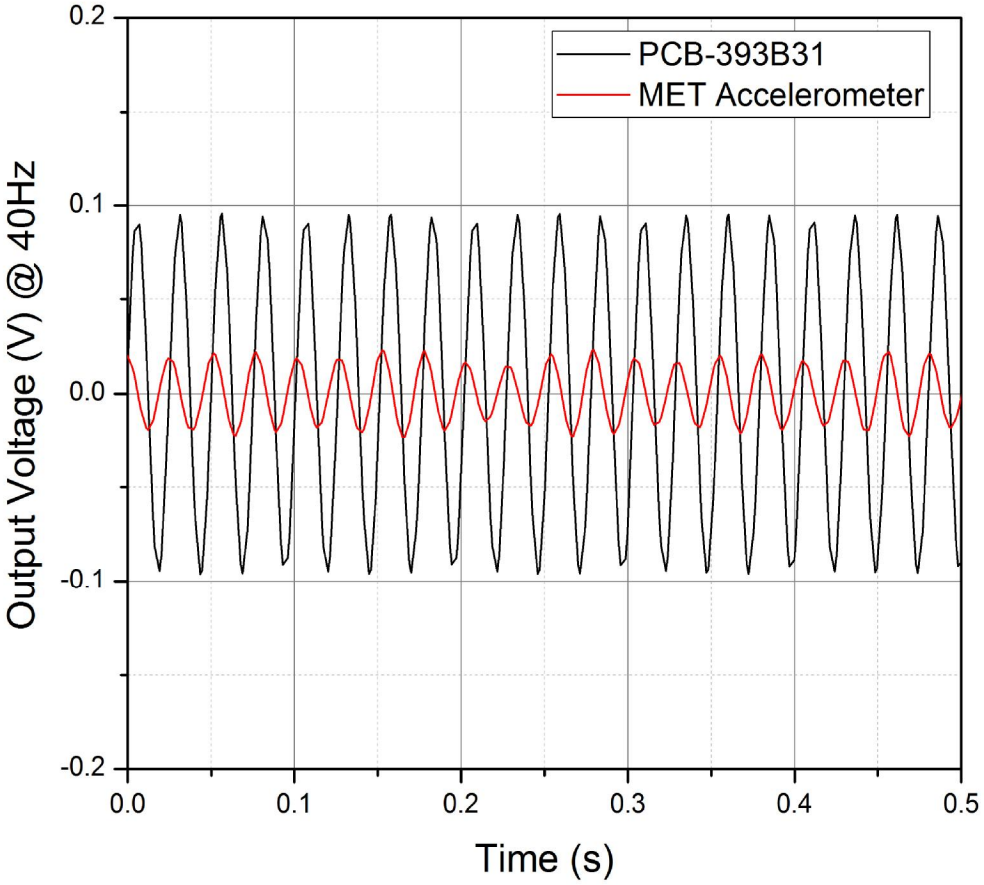

Figure 15. Comparison of voltage output of PCB 393B31 piezoelectric accelerometer and MET accelerometer

Amplitude linearity is a measure of how linear the output of an accelerometer is at a specific frequency, and also one of the key parameter of an accelerometer. Poor

amplitude linearity causes signal distortion especially in high amplitude accelerations. By tuning the gain, the MET accelerometer shows a good linearity sensitivity at frequency of 40 Hz as shown in Figure 16.

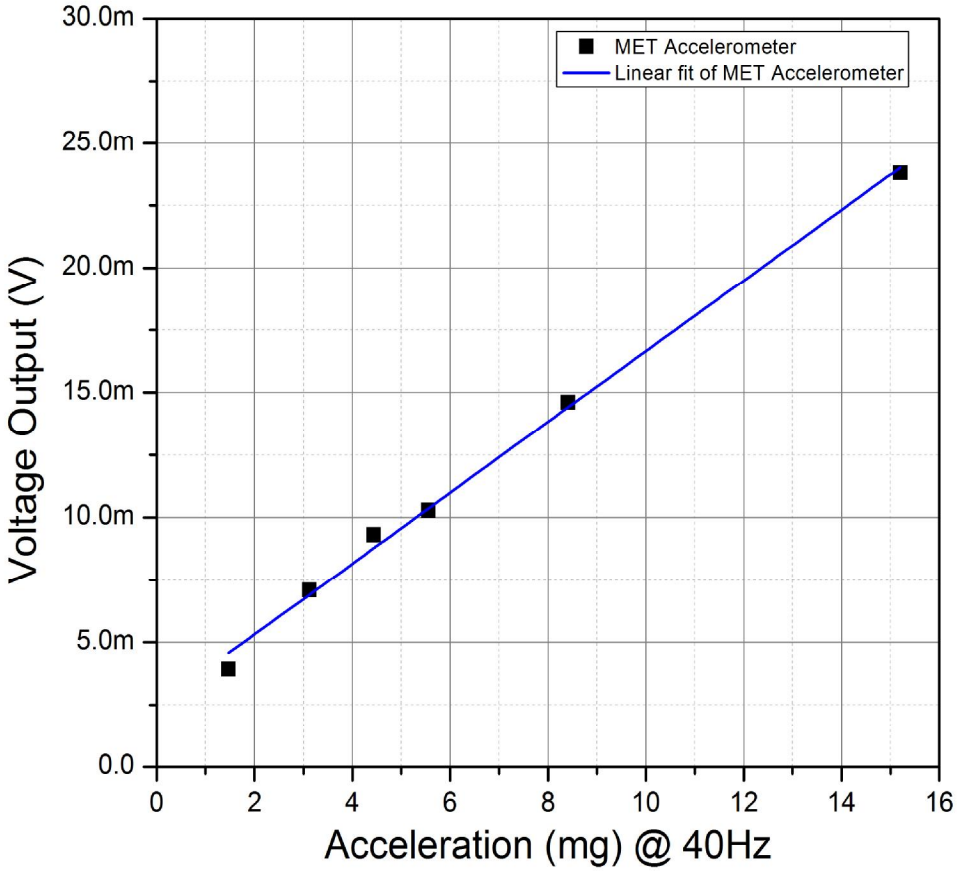

Figure 16. Amplitude linearity of MET accelerometer at 40 Hz.

As show in Figure 17, the frequency response of sensitivity of the MET accelerometer shows a peak sensitivity 10.4 V/G at 18 Hz and an almost flat response between 31 Hz to 60 Hz.

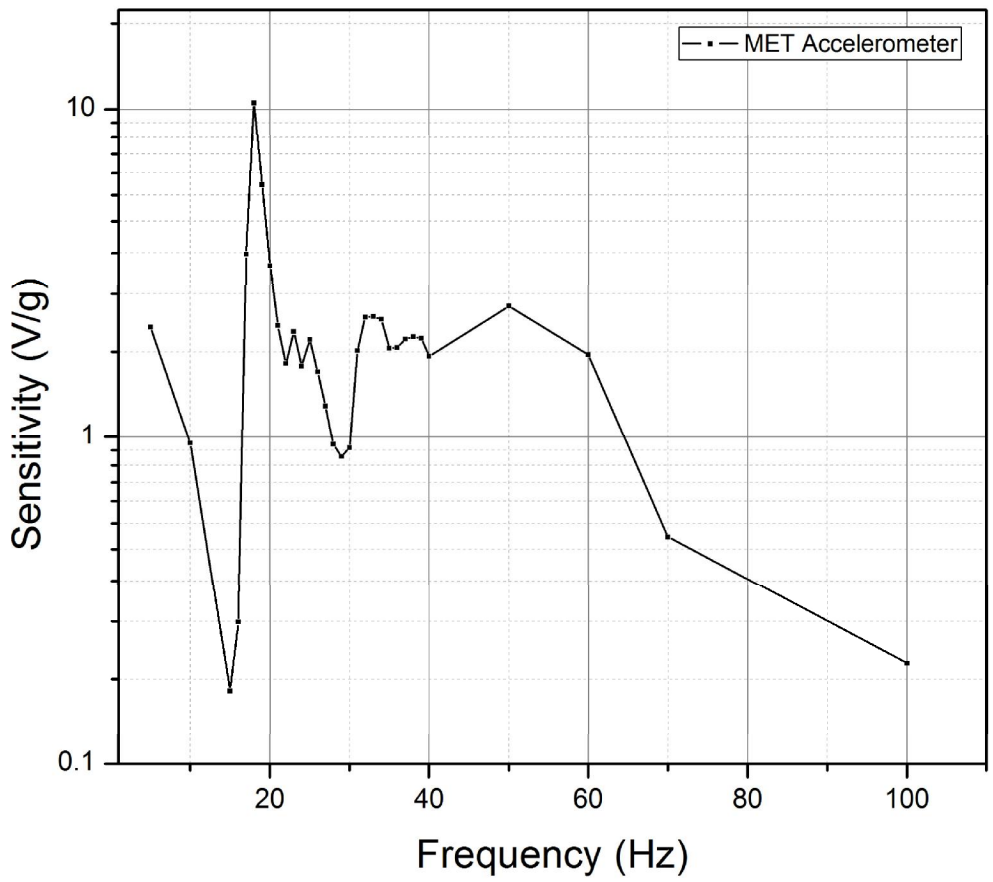

Figure 17. Frequency response of sensitivity of the MET accelerometer

Figure 18 shows the power spectra of MET accelerometer at 40 Hz. The power spectra are calculated from FFT of the accelerometer data in time domain. The input signal at 40 Hz has been clearly detected by the MET accelerometer, indicated by a peak at 40 Hz on its power spectra. Similar experiments have been performed on input signals ranging from 5 Hz to 100 Hz and input signal can be detected by this MET accelerometer from 18 to 70 Hz.

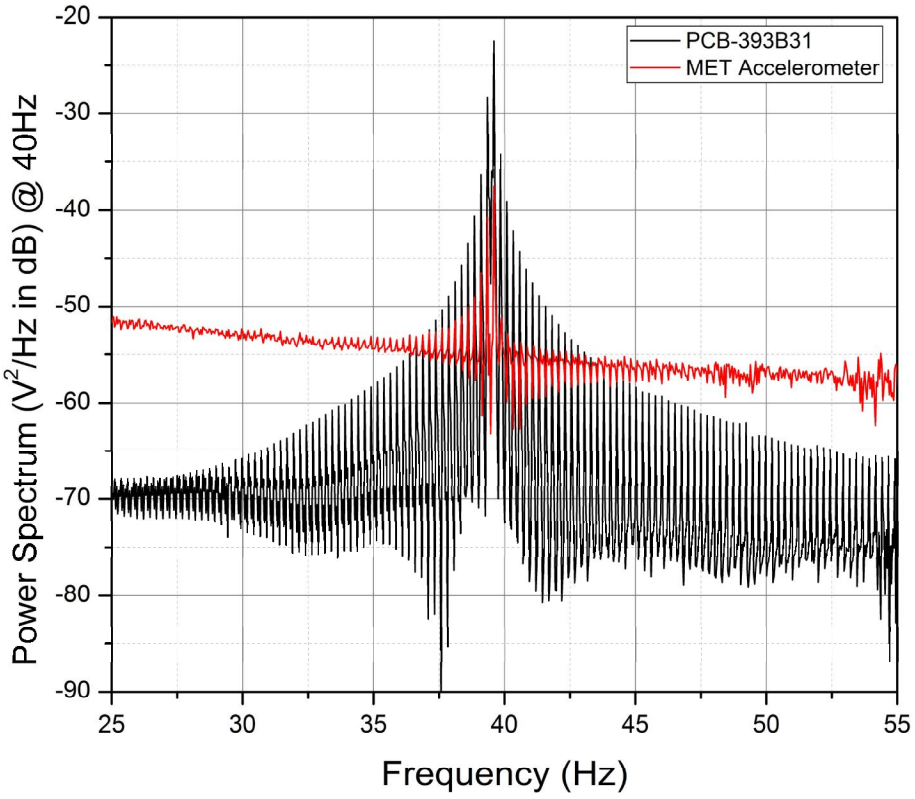

Figure 18. Power spectra of MET accelerometer at 40 Hz.

3.3. Noise Analysis

There are several sources of noise for MET accelerometer. Thermohydrodynamic noise, convection-induced noise and geometry noise usually are the main contributors.

The thermohydrodynamic noise comes from the fluctuations of the pressure difference on both sides of the channel of MET sensor. Although the liquid electrolyte is stable as a whole, there are local density variations (or fluctuations) in the liquid. And this causes the convection-induced noise. And the geometry noise is proportional to the electrochemical part of the transfer function of MET transducer and it dominates at very low frequency.

As shown in Figure 19, the noise for current design is high compared with high-performance MET sensor (CME-6211, noise is around -150 at 10 Hz). [8] It may come from electronic noise and thermohydrodynamic noise.

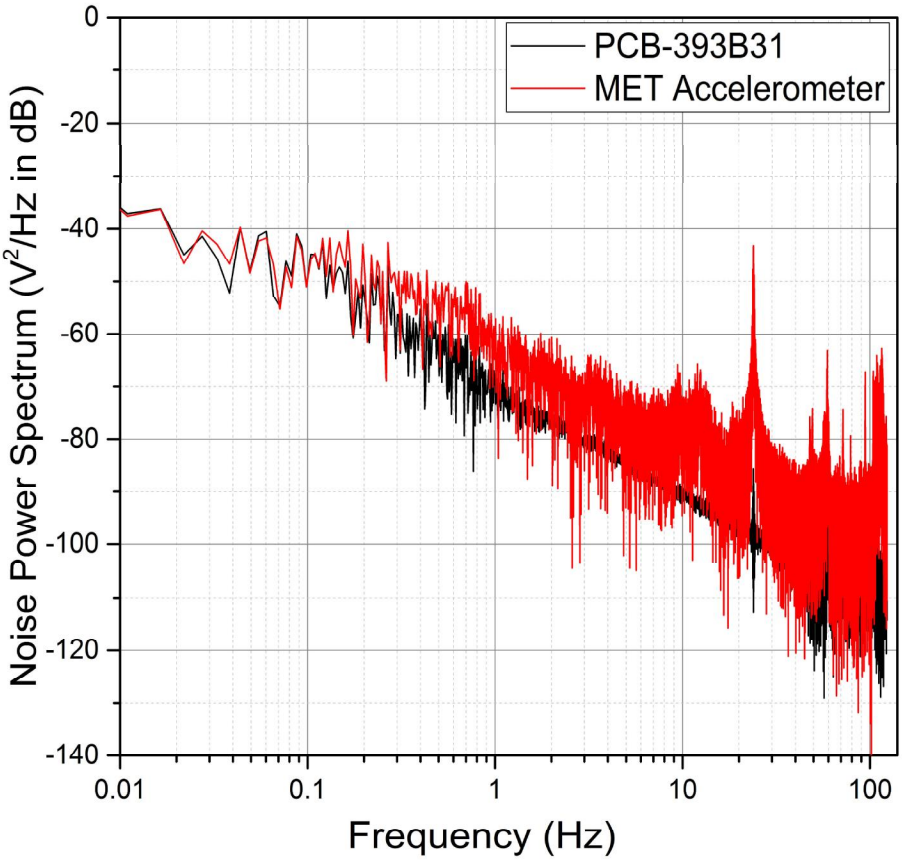

Figure 19. Noise Power spectra of MET accelerometer.

The electronic noise could be another source of the noise. Electronic noise in the MET sensor comes mostly from the signal conditioning circuits, including the current to voltage converter and filters. We can decrease the electronic noise by introducing a high impedance and conversion factor into the MET transducer. Also, low-noise operational amplifiers can also help. In MET devices, the electronic noise occurs at relatively high frequencies.

The thermohydrodynamic noise spectra density relates to the density of elelctrolyte and the hydrodynamic impedance of the transducer:

$$\langle a \rangle^2{}_{\omega} = \frac{2k_B \cdot T \cdot R_h}{\rho^2 L^2}$$

T is the temperature, k_B is Boltzmann's constant, ρ is the electrolyte density, L is the length of the transducer channel, R_h is the hydrodynamic impedance of the transducer which is proportional to the length of sensing element and the viscosity of the fluid. In current design, CuI saturated solution is used as the elelctrolyte. The solubility of CuI in water is 0.0042 g/100 mL, which is very low. This means the density of the electrolyte is pretty close to that of water, which are small. And the impedance of the electrolyte is also close to that of the water, which is high. Both may contribute to the noise in this MET sensor.

However as indicated by the equation, The thermohydrodynamic contribution of noise is independent of frequency. So it seems like the electronic noise is the main contributor of the noise in the MET sensor. Anyway, more experimental work need to be done before we can assure the source of noise in the MET sensor.

CHAPTER 4

SUMMARY AND FUTURE WORK

4.1 Summary

The focus of this thesis is on design, fabrication and testing results of the MET based accelerometer. Chapter 1 gives the basic ideas of microelectromechanical systems including its history and development are introduced. Then the working principle of accelerometers, taking capacitive accelerometer as an example, is demonstrated. However, solid-state mass-spring accelerometer has its intrinsic limitations. Therefore a new type of accelerometer based on liquid electrolytes - Molecular Electronic Transducer (MET) is introduced, In addition, the working principles of Molecular Electronic Transducer and Galvanic cell are introduced and discussed in detail in the last two sections of chapter 1. Furthermore, in Chapter 2, typical fabrication process for microelectromechanical system is introduced including bulk micromachining, surface micromachining, wet etching, isotropic and anisotropic, deep reactive ion etching and lift-off. Fabrication process for molecular electronic transducer is also demonstrated by taking MET accelerometer with droplet as sensing body as an example. As the technique with which molecular electronic transducer cell is created, 3D printing technique is introduced in this chapter. The history of 3D printing is described and a comparison between different 3D printing technologies is made. And Stereolithography (SLA) 3D printing technique is explained in detail. In Chapter 3, the experimental set-up for MET accelerometer has been described then experimental data of MET accelerometer is analyzed.

4.2 Future Work

As previously mentioned, this thesis focuses on the design, fabrication and testing results of the MET based accelerometer in Galvanic cell . However, the theoretical analysis of the mechanism of MET accelerometer based on complex electrochemical theory is not available yet. It would be interesting to see how FEA simulation (e.g. Comsol Multiphysics, Ansys) tell us about these MET accelerometers. Such simulations would help to do the parameter optimization for our experiments.

This thesis only studied a specific electrochemical reaction: Zn/Cu and CuI to show how this MET based accelerometer works. In reality, there will be many combinations available for such MET based accelerometers, for example Li battery with liquid electrolyte of high density and low impedance will be an interesting candidate for this purpose. So the goal is to find the combination with best performance with assistance from FEA simulation and then testify it with experiments.

REFERENCES

[1] C.T. Leondes, MEMS/NEMS Handbook Techniques and Applications, Springer, 2006.

[2] History of MEMS, Southwest Center for Microsystems Education: University of New Mexico.

[3] Karen Lightman, "MEMS and Sensor Trends, Smaller, Faster and Available to the mass Market", 2013.

[4] Hai Huang, Mengbing Liang, Rui Tang, Jonathon Oiler and Hongyu Yu, "Molecular Electronic Transducer-based Low-Frequency Accelerometer Fabricated with Post-CMOS Compatible Process Using Droplet as Sensing Body", IEEE Electron Device Letters, 34, 1304, 2013.

[5] Joel Voldman, Case Study: A Capacitive Accelerometer, Massachusetts Institute of Technology, 2007.

[6] M.-B. Liang, A Molecular Electronic Transducer based Low-Frequency Accelerometer with Electrolyte Droplet Sensing Body, M.S. Thesis, Arizona State University, Tempe, 2013.

[7] Gary K. Fedder, "MEMS Fabrication", ITC International Conference, 691, 2003.

[8] H. Huang, Molecular Electronic Transducer-Based Seismometer and Accelerometer Fabricated With Micro-Electro-Mechanical Systems Techniques, Ph. D. dissertation, Arizona State University, Tempe, 2014.

[9] MEMS, Design and Fabrication, Edited by Mohamed Gad-el-Hak, Taylor & Francis Group, LLC, 3-1, 2006.

[10] Andrew Marshall and Sreedhar Natarajan, SOI Design, Analog, Memory and Digital Techniques, Kluwer Academic Publishers, 2003.

[11] Charles W. Hull, "Apparatus for production of three-dimensional objects by stereolithography", US 4575330 A, 1986.

[12] "3D-printing multi-material objects in minutes instead of hours". Kurzweil Accelerating Intelligence. November, 2013.